Discrete-Time Modeling and Path-Tracking for a Wheeled Mobile Robot[1]

Modelado en Tiempo Discreto y Seguimiento de Trayectorias para un Robot Móvil Populsado por Ruedas

Martin Velasco Villa[*2], Eduardo Aranda Bricaire[**] and Rodolfo Orosco Guerrero[***]

[*]ESIME-Culhuacan, Instituto Politécnico Nacional
Av. Santa Ana 1000, 04430 México D.F., México.
velasco@cinvestav.mx

[**]CINVESTAV-IPN, Departamento de Ingeniería Eléctrica, Sección de Mecatrónica
Apdo. 14-740, 07000, México DF, México.
earanda@cinvestav.mx

[***]Instituto Tecnológico de Celaya, Departamento de Ingeniería Electrónica,
Av. Tecnológico y A. García S/N, Celaya Guanajuato, México.
rodolfoo@itc.mx

Article received on March 10, 2008; accepted on September 04, 2008

Abstract
The exact discrete-time model of a two wheel differentially driven mobile robot is obtained by direct integration of its continuous-time kinematic model. The discrete-time model obtained is used to design two discrete-time linearizing control laws with different singular manifolds. These control laws are used to propose a commutation control scheme that solves the path-tracking problem and guarantees internal stability of the closed loop system. The performance of the control scheme is evaluated by the real time implementation of the proposed control strategy over a laboratory prototype.
Keywords: Discrete-time systems, mobile robots, feedback linearization, real time systems.

Resumen
El modelo exacto en tiempo discreto de un robot móvil propulsado por diferencias de velocidades es obtenido por integración directa de su modelo cinemático en tiempo continuo. El modelo en tiempo discreto es utilizado para diseñar dos leyes de control por linealización por retroalimentación con diferentes variedades singulares. Estas leyes de control son usadas para proponer un esquema de control por conmutación que resuelve el problema de seguimiento de trayectoria y garantiza la estabilidad interna del sistema en lazo cerrado. El desempeño del esquema de control es evaluado mediante la implementación en tiempo real de la estrategia de control propuesta sobre un prototipo de laboratorio.
Palabras clave: Sistemas en tiempo discreto, robots móviles, linealización por retroalimentación, sistemas en tiempo real.

1 Introduction

Discretization of continuous-time systems is especially important for control purposes because in actual practice most controllers are digitally implemented and therefore operate in discrete time. As a matter of fact, if an exact discrete-time model is available and a discrete-time control law can be synthesized from this model, then the performance of the controller is independent of the sampling rate. Unfortunately, the exact discretization of a continuous time nonlinear system is not always possible. A nonlinear system can be exactly discretized only in the case when the continuous-time model subject to piecewise constant input (sampled input) can be analytically solved. It is shown below that the kinematic model of a wheeled mobile robot satisfies this remarkable property.

Feedback linearization is one of the control alternatives for nonlinear systems. There is a complete theory about this nonlinear control strategy [Isidori, 95; Nijmeijer and Van der Schaft, 90] dealing mainly with the continuous-time case. Several problems studied for the continuous-time case can also be stated on a discrete-time context [Kotta,

[1] First author work was partially supported by CONACyT-México, Under Grant 61713.
[2] M. Velasco-Villa is on sabbatical leave from CINVESTAV-IPN, México.

95]. However, the solutions obtained for continuous-time systems are not always parallel to the solutions obtained for discrete-time systems. For the study of nonlinear discrete-time systems, see Nijmeijer and Van der Schaft, 90, Chapter 14, or Kotta, 95 where the subject is treated more deeply. Also, for the discrete-time case, different notions of feedback linearization are studied in [Aranda et *al.*, 96].

The control of mobile robots in continuous time has been widely studied in the literature, see for instance [Campion et *al.*, 96] and [Canudas et *al.*, 96] where several control problems and structural properties have been treated respectively. Also, for the continuous time case, in [Aranda et *al.* 02; D'Andrea-Novel et al 92; Oriolo et *al.* ,02] the feedback linearization problem is considered for several types of mobile robots and, in particular, the case of a two wheel differentially driven mobile robot is boarded. The feedback linearization approach and its application to the path tracking problem for a trailer-like system was considered in [Orosco et *al.*, 92; Orosco et *al.*, 92a].

Most of the time, real time implementation of continuous-time control strategies is achieved on a DSP, PC or microcontroller, assuming that the sampling frequency is fast enough. The main drawback of this approach is that the performance of the control law depends on the sampling frequency. One possible way to overcome this issue is to consider the design of discrete-time control strategies. In the field of mobile robots, some attempts have been made in this direction. For instance, in [Corradini et *al.*, 99; Corradini et *al.*, 02] the robust stabilization and the trajectory tracking problems are considered using an approximate discrete-time model of a two wheel differentially driven mobile robot. Also, in [Wargui et *al.*, 96; Wargui et *al.*, 97] the approximate discrete time model of a mobile robot of the same type is used to solve the stabilization problem by means of a switching strategy. Considering a hybrid approach, the stabilization problem of a mobile robot is boarded in [Oelen et *al.*, 95].

In a certain sense, the methods that rely on an approximate discrete-time model (e.g. Euler approximations) suffer from the same problem as the digital implementation of a continuous-time control law, namely, they strongly depend on the sampling frequency.

The goals of this paper are three: First, in order to avoid the lack of robustness and poor performance of control schemes based on approximate models, an exact discrete-time model for a class of two wheels differentially driven mobile robot is obtained. Second, the path tracking problem for the discrete-time model is considered. The specific feature of our approach is the design of two linearizing control laws and a commutation policy which solves the path-tracking problem globally. Finally, the performance of the above mentioned control strategy is tested over a laboratory prototype.

The paper is organized as follows: In Section 2, the discretization of the continuous-time kinematic model of a two-wheel differentially driven mobile robot is obtained. In Section 3, the explicit design of a path-tracking control via feedback linearization and a switching strategy is developed. In Section 4, the stability analysis of the proposed control scheme is presented. Section 5 is devoted to the real time implementation of the developed strategy and its performance is shown by tracking a particular desired trajectory over the plane. Finally, some conclusions are presented in Section 6.

2 Discrete-time model

The type of wheeled mobile robot considered in this work is shown in Figure 1. This class of robots, called *two-wheel differentially driven mobile robot* consists of two parallel fixed wheels driven independently. A change of direction is obtained by the difference of velocity between the traction wheels. The continuous-time kinematic model of this mobile robot is well known in the literature [Campion et *al.*, 96; Canudas et *al.*, 96], and is given by

$$\begin{aligned} \dot{x}_1 &= u_1 \cos\theta_0 \\ \dot{x}_2 &= u_1 \sin\theta_0 \\ \dot{\theta}_0 &= u_2, \end{aligned} \tag{1}$$

where (x_1, x_2) represents the coordinates of the center of the axle of the actuated wheels on the plane (X_1, X_2) and θ_0 is the angle that the longitudinal axis of the robot forms with the axis X_1. The input signal u_1 represents the

longitudinal velocity of the robot and u_2 its angular velocity.

In what follows, it is shown that an exact discrete-time model for system (1) can be obtained by direct integration. Consider a constant sampling period T and define the time interval between two consecutive sampling instants as,

$$t_k = \{t \in \mathsf{R} \mid kT \le t < (k+1)T\}, \quad k = 0,1,2,\ldots$$

In the rest of the paper we assume that the control variables $u_1(t)$ and $u_2(t)$ remain constant between sampling instants (i.e. the inputs are sampled and connected to a zero order hold). Define $u_1(kT)$ and $u_2(kT)$ as the constant values that the input signals $u_1(t)$ and $u_2(t)$ take over the time intervals t_k for $k = 0,1,2,3,\ldots$.

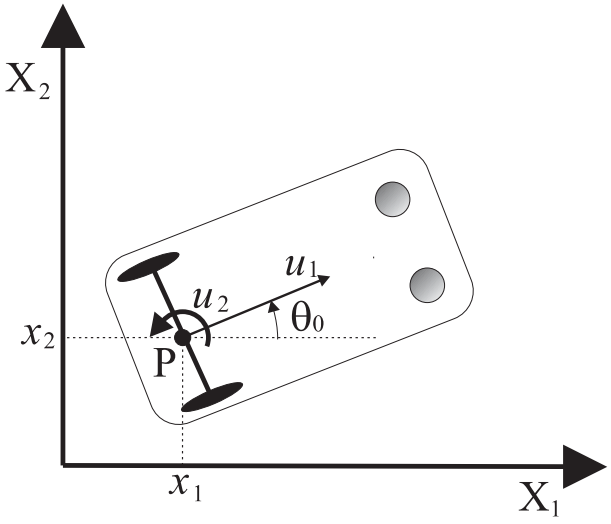

Fig. 1. Two-wheel differentially driven mobile robot

The equivalent discrete-time model for system (1) can be obtained by its direct integration over the interval t_k. Considering first the evolution of $\theta_0(t)$ on equation (1), one readily obtains,

$$\theta_0(t) = \theta_0(kT) + (t - kT)u_2(kT), \tag{2}$$

for $t \in t_k$. Integrating now the first equation in (1) with $\theta_0(t)$ given as in (2) produces,

$$x_1(t) \;=\; x_1(kT) + u_1(kT)\int_{kT}^{t} \cos\big(\theta_0(kT) + (\tau - kT)u_2(kT)\big)\,d\tau,$$

that leads to,

$$x_1(t) \;=\; x_1(kT) + \frac{u_1(kT)}{u_2(kT)}[-\sin\theta_0(kT) + \sin\big(\theta_0(kT) + (t - kT)u_2(kT)\big)], \tag{3}$$

for $t \in t_k$. Finally, from the second equation of (1) with $\theta_0(t)$ as in (2) we obtain

$$x_2(t) = x_2(kT) + u_1(kT)\int_{kT}^{t} \sin\big(\theta_0(kT) + (\tau - kT)u_2(kT)\big)d\tau,$$

that, evaluating the integral produces,

$$x_2(t) = x_2(kT) + \frac{u_1(kT)}{u_2(kT)}[\cos\theta_0(kT) - \cos\big(\theta_0(kT) + (t - kT)u_2(kT)\big)], \tag{4}$$

for $t \in t_k$. In order to obtain the discrete-time model of the wheeled mobile robot (1), the equations (2), (3) and (4) are evaluated at the end of the interval t_k , this is,

$$\begin{aligned} x_1(kT+T) &= x_1(kT) + \frac{u_1(kT)}{u_2(kT)}\big[-\sin\theta_0(kT) + \sin\big(\theta_0(kT) + Tu_2(kT)\big)\big] \\ x_2(kT+T) &= x_2(kT) + \frac{u_1(kT)}{u_2(kT)}\big[\cos\theta_0(kT) - \cos\big(\theta_0(kT) + Tu_2(kT)\big)\big] \\ \theta_0(kT+T) &= \theta_0(kT) + Tu_2(kT). \end{aligned} \tag{5}$$

For the sake of simplicity, in the rest of the paper, the following notation is adopted $\zeta = \zeta(kT)$, $\zeta^{\pm} = \zeta(kT \pm T)$ and $\zeta^{[\pm i]} = \zeta(kT \pm iT)$. Using this notation and by means of simple algebraic manipulations, system (5) can be rewritten as,

$$\begin{aligned} x_1^{+} &= x_1 + 2u_1\psi(u_2)\cos\gamma(\theta_0, u_2) \\ x_2^{+} &= x_2 + 2u_1\psi(u_2)\sin\gamma(\theta_0, u_2) \\ \theta_0^{+} &= \theta_0 + u_2T, \end{aligned} \tag{6}$$

Where

$$\psi(u_2) = \begin{cases} \dfrac{\sin\left(\frac{T}{2}u_2\right)}{u_2} & \text{if } u_2 \neq 0 \\ \dfrac{T}{2} & \text{if } u_2 = 0, \end{cases}, \quad \gamma(\theta_0, u_2) = \theta_0 + \frac{T}{2}u_2.$$

Remark 2.1 *Note that the function* ψ *satisfies,* $\lim_{u_2 \to 0}\psi(u_2) = \frac{T}{2}$ *. In particular, when* $u_2 = 0$ *the state* θ_0 *remains constant accordingly to the property of the continuous-time model (1). It is easy to verify that the discrete-time model obtained from (1) when* $u_2 = 0$ *corresponds to the discrete-time model (6) with* $\psi(0) = \frac{T}{2}$

3 Discrete-time control scheme

In this section, the design of a commutation strategy for system (6) is developed. The control strategy achieves the path-tracking of a desired trajectory for the mobile robot based on the commutation between two discrete-time

nonlinear control laws. Both control laws linearize the input/output response of the system with respect to different output functions. The first output function possesses trivial zero dynamics. Therefore, the corresponding control law fully linearizes the system. The second output function exhibits zero dynamics of dimension one. The two output functions possess different singular manifolds. Therefore, a control switching strategy allows to construct a globally defined control law.

In the continuous-time case, a nonlinear control via feedback linearization for the mobile robot (1) is commonly based on the output function $h(x)=[x_1,x_2]^T$. However, the consideration of this output function in the discrete-time case (6) does not produce the same result, it is a straightforward task to prove that, in this case, it is obtained an input-output linearization with unstable zero dynamics.

3.1 Dynamic extension

In order to obtain an equivalent control scheme that the one produced by considering $h(x)=[x_1,x_2]^T$ in the continuous-time case, consider now, for the discrete-time counterpart, the output function,

$$y=\begin{bmatrix}\bar{h}_1(x,\theta_0,\theta_0^-)\\ \bar{h}_2(x,\theta_0,\theta_0^-)\end{bmatrix}=\begin{bmatrix}x_1\sin\frac{\theta_0+\theta_0^-}{2}-x_2\cos\frac{\theta_0+\theta_0^-}{2}\\ \theta_0^-\end{bmatrix}. \tag{7}$$

Notice that this output function depends on the current and past values of θ_0. In order to construct an output function defined only in terms of a classical realization it is necessary to define θ_0^- as a new state, this is done by means of the following dynamic extension,

$$\xi_1^+=\theta_0. \tag{8}$$

Therefore, for the augmented system (6)-(8) the output (7) is rewritten as

$$y=\begin{bmatrix}\bar{h}_1(x,\theta_0,\xi_1)\\ \bar{h}_2(x,\theta_0,\xi_1)\end{bmatrix}=\begin{bmatrix}x_1\sin\frac{\theta_0+\xi_1}{2}-x_2\cos\frac{\theta_0+\xi_1}{2}\\ \xi_1.\end{bmatrix}. \tag{9}$$

System (6)-(8) with output function (7) possess a singular decoupling matrix [Kotta, 95; Nijmeijer and Van der Schaft, 90]. Therefore, in order to linearize the input/output response, it is proposed the dynamic extension,

$$\begin{aligned}u_2 &= \xi_2,\ \ \xi_2^+=w_2,\\ u_1 &= w_1,\end{aligned} \tag{10}$$

where w_1, w_2 are new control inputs. This allows to rewrite (6)-(8)-(10) as the extended system,

$$x^+=f(x,w), \tag{11}$$

where, $x=[x_1,x_2,\xi_1,\theta_0,\xi_2]^T$, $w=[w_1,w_2]^T$ and,

$$f(x,w)=\begin{bmatrix} x_1+2\psi(\xi_2)w_1\cos\gamma(\theta_0,\xi_2) \\ x_2+2\psi(\xi_2)w_1\sin\gamma(\theta_0,\xi_2) \\ \theta_0 \\ \theta_0+T\xi_2 \\ w_2 \end{bmatrix},\quad \psi(\xi_2)=\frac{\sin\left(\frac{T}{2}\xi_2\right)}{\xi_2},\quad \gamma(\theta_0,\xi_2)=\theta_0+\frac{T}{2}\xi_2.$$

Remark 3.1 *The dynamic extension (8)-(10) depicted in Figure 2 amounts to add one pure time delay in front of the input* u_2*, and to store the value at the previous time instant of the variable* θ_0*, in order to synthesize the linearizing control law.*

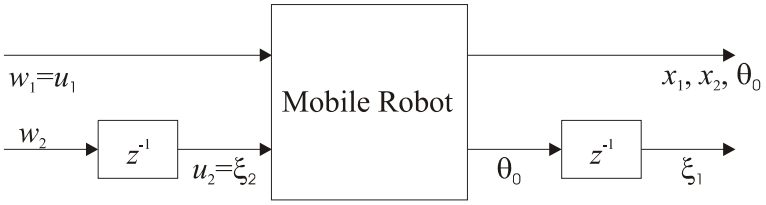

Fig.2. Extended System (11)

3.2 Design of full linearizing control law

In order to solve the path tracking problem, consider now the augmented system (11) and the output function (9). It is possible to compute for the component $\bar{h}_1$,

$$\begin{aligned} y_1 &= \bar{h}_1(x)= x_1\sin\left(\tfrac{\theta_0+\xi_1}{2}\right)- x_2\cos\left(\tfrac{\theta_0+\xi_1}{2}\right) \\ y_1^+ &= \bar{h}_1^+(x)= x_1\sin\gamma - x_2\cos\gamma \\ y_1^{[2]} &= \bar{h}_1^{[2]}(x,w)= x_1\sin\gamma^+ - x_2\cos\gamma^+ - 2\psi(\xi_2)w_1\sin\left(\gamma-\gamma^+\right) \end{aligned}$$

where $\gamma^+=\theta_0+T\xi_2+\frac{T}{2}w_2$. For the output component $\bar{h}_2$, the first three forward shifts are given by

$$\begin{aligned} y_2 &= \bar{h}_2(x)= \xi_1 \\ y_2^+ &= \bar{h}_2^+(x)= \theta_0 \\ y_2^{[2]} &= \bar{h}_2^{[2]}(x)= \theta_0+T\xi_2 \\ y_2^{[3]} &= \bar{h}_2^{[3]}(x,w)= \theta_0+T\xi_2+Tw_2. \end{aligned}$$

Considering the functions $y_1^{[2]}(x,w)$, $y_2^{[3]}(x,w)$ it is possible to write,

$$\begin{bmatrix} y_1^{[2]} \\ y_2^{[3]} \end{bmatrix} = \begin{bmatrix} \bar{h}_1^{[2]} \\ \bar{h}_2^{[3]} \end{bmatrix}= \begin{bmatrix} x_1\sin\gamma^+ - x_2\cos\gamma^+ \\ \theta_0+T\xi_2 \end{bmatrix}+\begin{bmatrix} -2\psi(\xi_2)\sin\left(\gamma-\gamma^+\right) & 0 \\ 0 & T \end{bmatrix}\begin{bmatrix} w_1 \\ w_2 \end{bmatrix}.$$

From the last equations, it is clear that the decoupling matrix

$$D = \begin{bmatrix} -2\psi(\xi_2)\sin\left(\gamma - \gamma^+\right) & 0 \\ 0 & T \end{bmatrix},$$

becomes singular on the manifold

$$\bar{S} = \left\{ (x,\xi) \in \mathsf{R}^5 \mid \xi_2 + w_2 = \pm\frac{2n\pi}{T} \text{ or } \xi_2 = \pm\frac{2m\pi}{T}, \quad n = 0,1,2..., \; m = 1,2..... \right\}. \tag{12}$$

Finally a feedback control law that solves the path tracking problem is given by

$$\begin{bmatrix} w_1 \\ w_2 \end{bmatrix} = \begin{bmatrix} \dfrac{1}{2\psi\sin\left(\frac{\theta_0 - v_2}{2}\right)}(x_1\sin\phi - x_2\cos\phi - v_1) \\ \dfrac{1}{T}(v_2 - \theta_0 - T\xi_2) \end{bmatrix}, \tag{13}$$

where $\phi = \frac{v_2 + \theta_0 + T\xi_2}{2}$ and the new input variables v_1 and v_2 are,

$$\begin{aligned} v_1 &= y_{1d}^{[2]} - \bar{k}_1 e_1^+ - \bar{k}_0 e_1 \\ v_2 &= y_{2d}^{[3]} - \bar{m}_2 e_2^{[2]} - \bar{m}_1 e_2^+ - \bar{m}_0 e_2 \end{aligned} \tag{14}$$

with the output error $e_i = y_i - y_{id}$.

For the sake of conciseness, in the rest of the paper the control law (13)-(14) designed for system (11), will be referred to as $\bar{w}$. For the closed loop system (11)-(13)-(14), the tracking error dynamics is governed by the difference equations

$$\begin{aligned} e_1^{[2]} + \bar{k}_1 e_1^+ + \bar{k}_0 e_1 &= 0 \\ e_2^{[3]} + \bar{m}_2 e_2^{[2]} + \bar{m}_1 e_2^+ + \bar{m}_0 e_2 &= 0. \end{aligned} \tag{15}$$

Remark 3.2 *The relative degrees of system (11)-(9) are* $\bar{r}_1 = 2$, $\bar{r}_2 = 3$ *and their sum is equal to the dimension of the extended system (11), then feedback law (13) fully linearizes the system.*

Remark 3.3 *The control law* $\bar{w}$ *is undefined on the singular manifold* $\bar{S}$ *given in (12).*

3.3 Complementary feedback law

Since $\bar{w}$ is not defined on $\bar{S}$, in order to obtain a global control scheme, an alternative control law with a different singular manifold is proposed. This alternative control law can be enabled when the state is in a neighborhood of $\bar{S}$. To obtain this second feedback consider now the output function,

$$\tilde{y} = \begin{bmatrix} \tilde{h}_1(x,\theta_0,\xi_1) \\ \tilde{h}_2(x,\theta_0,\xi_1) \end{bmatrix} = \begin{bmatrix} x_1\cos\left(\frac{\theta_0+\xi_1}{2}\right) + x_2\sin\left(\frac{\theta_0+\xi_1}{2}\right) \\ \xi_1 \end{bmatrix}. \tag{16}$$

Applying the same procedure as in the previous section it is obtained,

$$\begin{bmatrix} \tilde{y}_1^+ \\ \tilde{y}_2^{[3]} \end{bmatrix} = \begin{bmatrix} \tilde{h}_1^+ \\ \tilde{h}_2^{[3]} \end{bmatrix} = \begin{bmatrix} x_1 \cos\gamma + x_2 \sin\gamma \\ \theta_0 + T\xi_2 \end{bmatrix} + \begin{bmatrix} 2\psi & 0 \\ 0 & T \end{bmatrix} \begin{bmatrix} w_1 \\ w_2 \end{bmatrix}.$$

In this case, the decoupling matrix

$$\tilde{D} = \begin{bmatrix} 2\psi(\xi_2) & 0 \\ 0 & T \end{bmatrix}$$

becomes singular on the manifold

$$\tilde{S} = \left\{ (x, \xi) \in \mathsf{R}^5 \mid \xi_2 = \pm \frac{2m\pi}{T}, \quad m = 1, 2, \ldots \right\}. \tag{17}$$

When the state does not belong to the manifold $\tilde{S}$, it is possible to synthesize the feedback law,

$$\begin{bmatrix} w_1 \\ w_2 \end{bmatrix} = \begin{bmatrix} \frac{1}{2\psi}(\tilde{v}_1 - x_1 \cos\gamma - x_2 \sin\gamma) \\ \frac{1}{T}(\tilde{v}_2 - \theta_0 - T\xi_2) \end{bmatrix} \tag{18}$$

where $\tilde{v}_1$ and $\tilde{v}_2$ are given as,

$$\begin{aligned} \tilde{v}_1 &= \tilde{y}_{1d}^+ - \tilde{k}_0 \tilde{e}_1 \\ \tilde{v}_2 &= \tilde{y}_{2d}^{[3]} - \tilde{m}_2 \tilde{e}_2^{[2]} - \tilde{m}_1 \tilde{e}_2^+ - \tilde{m}_0 \tilde{e}_2. \end{aligned} \tag{19}$$

with the output error $\tilde{e}_i = \tilde{y}_i - \tilde{y}_{id}$.

Again, for sake of conciseness the control law (18)-(19) designed for system (11) will be referred to as $\tilde{w}$. In this case, the closed loop system (11)-(18)-(19) produces the tracking error dynamics

$$\begin{aligned} \tilde{e}_1^+ + \tilde{k}_0 \tilde{e}_1 &= 0 \\ \tilde{e}_2^{[3]} + \tilde{m}_2 \tilde{e}_2^{[2]} + \tilde{m}_1 \tilde{e}_2^+ + \tilde{m}_0 \tilde{e}_2 &= 0. \end{aligned} \tag{20}$$

Remark 3.4 *The relative degrees of system (11)-(16) are* $\tilde{r}_1 = 1$, $\tilde{r}_2 = 3$ *and their sum is equal to four, therefore the extended system (11) under the control law (18) possesses a zero dynamics of dimension one.*

Remark 3.5 *The control law* $\tilde{w}$ *is not defined when the state belongs to the singular manifold* $\tilde{S}$ *given in (17).*

3.4 Commutation strategy

The control scheme proposed in this subsection is based on the commutation between control laws $\bar{w}$ and $\tilde{w}$ defined by (13)-(14) and (18)-(19), respectively. The singularities on the feedback (18) appear when the angular

velocity of the robot ξ_2 is equal to a multiple of the sampling frequency (17), i.e., $\xi_2 = \pm\frac{2m\pi}{T}$. For most sampling periods considered for practical discrete-time applications ($T << 1\text{s}$), these singularities can only appear for very high angular velocities of the mobile robot. Therefore, it can be reasonably assumed that this singularity does not appear in practical robots. For these reasons it is proposed a commutation strategy that mainly takes into account the singularities produced by $\bar{S}$ instead of $\tilde{S}$. The commutation strategy takes the form,

$$w = \begin{cases} \bar{w}, & \text{if } \left|\xi_2 + \bar{w}_2\right| \geq \dfrac{2m\pi}{T} + \varepsilon \\ \tilde{w}, & \text{if } \left|\xi_2 + \bar{w}_2\right| < \dfrac{2m\pi}{T} + \varepsilon \end{cases} \quad m = 0,1,2,\ldots \tag{21}$$

where ε is a small positive number that represents the commutation threshold. From the properties of the singular manifolds $\bar{S}$ and $\tilde{S}$ explained above, the proposed strategy enables the control law $\bar{w}$ most of the time, and the feedback control law $\tilde{w}$ is intended to act only when the state is on the neighborhood of the singularity $\xi_2 + \bar{w}_2 = \pm\frac{2m\pi}{T}$.

Remark 3.6 *One remarkable feature of the discrete-time setting is that the commutation scheme (21) preserves existence and uniqueness of the solutions of system (11). It is well known that this is not necessarily the case for continuous time systems when they are subject to discontinuous control laws.*

4 Stability analysis

This section is devoted to the analysis of the stability the closed-loop system composed by the extended system (11) and the control scheme (21) developed in the previous section. The control scheme (21) is based on the commutation between the full linearizing control law $\bar{w}$ and the input-output linearizing control law $\tilde{w}$.

The commutation scheme is designed in such a way that the control $\tilde{w}$ is enabled when the trajectories of the closed-loop system are in the neighborhood of the singular manifold $\bar{S}$. When this happens, it is possible to prove that the unobservable dynamics remains bounded. On the other hand, when $\bar{w}$ is enabled, the internal dynamics vanishes and then the closed-loop system (11)-(21) asymptotically follows the reference trajectory $\bar{y}_d(t)$. Combining the results announced above, it is possible to establish sufficient conditions for the stability of the closed-loop system (11)-(21).
In order to state the main result of this section, consider the following set of assumptions:

Assumption 4.1 *Coefficients $\bar{k}_i$, $\tilde{k}_i$, $\bar{m}_i$ and $\tilde{m}_i$ are such that the roots of the polynomials (15) and (20) are different and lie on the interval $(0,1)$.*

Assumption 4.2 *The function $r_k = \sqrt{\tilde{y}_{1d}^2 + \bar{y}_{1d}^2}$ belongs to the space of functions $P^n = \left\{p_k : \mathsf{Z} \to \mathsf{R} \,|\, |p_k| \leq a + bk^n\right\}$, where a and b are positive real.*

Assumption 4.3 *The trajectories of the closed-loop system (11)-(21) produce a finite number of commutations of the control scheme (21).*

Remark 4.4 *The function r_k represents the distance of the desired trajectory to the origin, i.e., $r_k = \sqrt{x_{1d}^2 + x_{2d}^2}$. Also note that Assumption 4.2 is far from been restrictive since r_k is bounded by a polynomial that can grow arbitrarily fast.*

Remark 4.5 *Note that Assumption 4.3 implies that there exists a positive number* k_0 *such that for all* $k \geq k_0$ *one of the control laws* $\bar{w}$ *or* $\tilde{w}$ *remains enabled.*

In the rest of the Section, $\|\cdot\|$ denotes the usual Euclidean norm, and by abuse of notation it also denotes the corresponding induced matrix norm. Also, $\lambda_i\{A\}$ denotes the set of eigenvalues of matrix A.
Before presenting the main result of the paper, some technical results are to be proven.

Lemma 4.6 *The mapping* $\Psi : \mathsf{R}^5 \to \mathsf{R}^5$ *defined by*

$$\hat{x} = \Psi(x) = \begin{bmatrix} \xi_1 \\ \theta_0 \\ \theta_0 + T\xi_2 \\ x_1 \cos\gamma + x_2 \sin\gamma \\ x_1 \sin\gamma - x_2 \cos\gamma \end{bmatrix}$$

where $\hat{x} = \left[\tilde{y}_2, \tilde{y}_2^+, \tilde{y}_2^{[2]}, \tilde{y}_1, \bar{y}_1\right]^T$ *and* $\gamma = \theta_0 + \frac{T}{2}\xi_2$, *is globally invertible and hence qualifies as global change of coordinates.*

Proof. Note that $x = \Psi^{-1}(\hat{x})$ is given by,

$$x = \Psi^{-1}(\hat{x}) = \begin{bmatrix} \tilde{y}_1 \cos\hat{\gamma} + \bar{y}_1 \sin\hat{\gamma} \\ \tilde{y}_1 \sin\hat{\gamma} - \bar{y}_1 \cos\hat{\gamma} \\ \tilde{y}_2 \\ \tilde{y}_2^+ \\ \frac{\tilde{y}_2^{[2]} - \tilde{y}_2^+}{T} \end{bmatrix}$$

where $\hat{\gamma} = \frac{\tilde{y}_2^+ + \tilde{y}_2^{[2]}}{2}$. Taking into account that $T \neq 0$, then the transformation $\Psi(x)$ is globally invertible.

Lemma 4.7 *Consider the discrete time system,*

$$x^+ = Ax. \tag{22}$$

Assume that $\lambda_i\{A\}$ *are real and different. Then, the solution of system (22) is bounded by*

$$\|x(k)\| \leq \gamma |\lambda_m|^k \|x(0)\|$$

where $\lambda_m = \max\{\lambda_i\{A\}\}$, $\gamma = \|P\|\|P^{-1}\|$ *and* P *is a matrix formed by the eigenvectors of matrix* A.

Proof. The proof is elementary and is left to the reader.

Lemma 4.8 *Consider the closed-loop system composed by the extended system (11) and the commutation scheme*

(21) and that Assumptions 4.1 and 4.2 are satisfied. Suppose that the control law $\tilde{w}$ *is enabled for all* $k \geq 0$. *Then, the tracking error* $\tilde{e}$ *converges asymptotically to zero, and the error* e_1 *is bounded by a suitable constant.*

Proof. Defining error variables $z = \hat{x} - \hat{x}_d = \Psi(x) - \Psi(x_d)$, the closed loop system (11)-(18) can be rewritten in z-coordinates as,

$$\begin{aligned} z_1^+ &= z_2 \\ z_2^+ &= z_3 \\ z_3^+ &= -\tilde{m}_2 z_3 - \tilde{m}_1 z_2 - \tilde{m}_0 z_1 \\ z_4^+ &= \tilde{k}_0 z_4 \\ z_5^+ &= z_5 \cos(z_\phi + \phi_d) + z_4 \sin(z_\phi + \phi_d) + 2r_k \sin\left(\frac{z_\phi}{2} + \phi_d + \tan^{-1}\left(\frac{\tilde{y}_{1d}}{y_{1d}}\right)\right)\sin\frac{z_\phi}{2}, \end{aligned} \tag{23}$$

where $\phi_d = \frac{\tilde{y}_{2d}^{[2]} - \tilde{y}_{2d}}{2}$, $z_\phi = \frac{z_3 - z_1}{2}$ and $r_k = \sqrt{\tilde{y}_{1d}^2 + y_{1d}^2}$.

Consider now the linear subsystem of (23),

$$\tilde{z}^+ = \tilde{A}\tilde{z}, \tag{24}$$

with, $\tilde{z} = [z_1, z_2, z_3, z_4]^T$ and,

$$\tilde{A} = \begin{bmatrix} 0 & 1 & 0 & 0 \\ 0 & 0 & 1 & 0 \\ -\tilde{m}_0 & -\tilde{m}_1 & -\tilde{m}_2 & 0 \\ 0 & 0 & 0 & \tilde{k}_0 \end{bmatrix}.$$

Under Assumption 4.1 and using Lemma 4.7, the solution of (24) is bounded by,

$$\|\tilde{z}(k)\| \leq \gamma |\lambda_m|^k \|\tilde{z}(0)\|$$

where $\gamma = \|\tilde{P}\|\|\tilde{P}^{-1}\|$ and the columns of $\tilde{P}$ are given by the characteristic vectors of $\tilde{A}$ and $\lambda_m = \max \lambda\{\tilde{A}\}$. Under this condition $\tilde{z}(k)$ converges asymptotically to zero and therefore $\tilde{e}(k)$ converges to zero.
From the nonlinear subsystem of (23), the state equation of z_5 can be rewritten as

$$z_5^+ = g_k z_5 + f_k, \tag{25}$$

where $g_k = \cos(z_\phi + \phi_d)$ and $f_k = z_4 \sin(z_\phi + \phi_d) + 2r_k \sin\left(\frac{z_\phi}{2} + \phi_d + \tan^{-1}\frac{\tilde{y}_{1d}}{y_{1d}}\right)\sin\frac{z_\phi}{2}$.

It is easy to see that the solution of (25) is given by,

$$z_5(k) = \left(\prod_{i=0}^{k-1} g_i\right) z_5(0) + \sum_{i=0}^{k-2}\left(\prod_{j=i+1}^{k-1} g_j\right) f_i + f_{k-1}. \tag{26}$$

Noting that $\|g_k\| \leq 1$, and using again simple norm properties one obtains

$$|z_5(k)| \leq |z_5(0)| + \sum_{i=0}^{k-1} |f_i|. \tag{27}$$

Now, from the fact that $|\sin(\alpha)| \leq 1$,

$$|f_i| \leq |z_4(i)| + 2r_i \left| \sin \frac{z_\phi(i)}{2} \right|.$$

Since $\left|\sin \frac{z_\phi}{2}\right| \leq \left|\frac{z_\phi}{2}\right|$, and noting that under Assumption 4.2, $r_i \leq a + bi^n$; it is obtained,

$$|f_i| \leq |z_4(i)| + \left(a + bi^n\right)|z_\phi|. \tag{28}$$

Equation (28) can be simplified further by noting that

$$|z_4(i)| \leq \|\tilde{z}(k)\| \leq \gamma K_0 |\lambda_m|^i, \quad |z_\phi(i)| \leq \frac{|z_3(k)| + |z_1(k)|}{2} \leq \|\tilde{z}(k)\| \leq \gamma K_0 |\lambda_m|^i$$

where $K_0 = |\tilde{z}(0)|$. This is,

$$|f_i| \leq \left(1 + a + bi^n\right) \gamma K_0 |\lambda_m|^i.$$

From the above developments, equation (27) is rewritten as,

$$|z_5(k)| \leq |z_5(0)| + (1+a)\gamma K_0 \sum_{i=0}^{k-1} |\lambda_m|^i + b\gamma K_0 \sum_{i=0}^{k-1} i^n |\lambda_m|^i.$$

From elementary calculus, it is clear that,

$$\sum_{i=0}^{k-1} |\lambda_m|^i \leq \frac{1}{1-|\lambda_m|}, \quad \sum_{i=0}^{k-1} i^n |\lambda_m|^i \leq C,$$

where C is a positive constant. Therefore,

$$|z_5(k)| \leq |z_5(0)| + \frac{(1+a)K_0}{1-|\lambda_m|} + bK_0 C,$$

from where it is concluded that $\tilde{e}_1$ is bounded.

Lemma 4.9 *Consider the closed-loop system composed by the extended system (11) and the commutation scheme (21). Suppose that the control law $\bar{w}$ is enabled for all $t \geq 0$. Then the tracking error $\tilde{e}$ converges asymptotically to zero.*

Proof. Since the control law $\overline{w}$ is enabled for all $t \geq 0$, then the dynamics of $\overline{e}$ is governed by equations (15). Since the corresponding characteristic polynomials are Schur (discrete-time Hurwitz), the results follows.

Now it is possible to present the main result of the paper:

Theorem 4.10 *Consider the closed-loop system composed by the extended system (11) and the commutation scheme (21). Suppose that Assumptions 4.1, 4.2 and 4.3 are satisfied. Then, one of the following assertions does hold:*

1) The error $\tilde{e}$ converges asymptotically to zero and the error $\overline{e}_1$ is bounded by a suitable constant.

2) The error $\overline{e}$ converges asymptotically to zero.

Proof. Since the closed-loop system is time-invariant, Lemmas 4.8 and 4.9 can be applied after each commutation by shifting the time-axis. Since only a finite number of commutations occur, one and only one of the assertions of Theorem 4.10 can arise. This concludes the Proof.

Remark 4.11 *The vector $\hat{x}$ is composed by the states controlled by the closed-loop system (11)-(18) and the state y_1. Therefore, y_1 can be considered as internal dynamics of the closed loop system.*

5 Real-time implementation

In this Section the performance of the commutation control scheme presented in the preceding Section is evaluated by its implementation over a low cost laboratory prototype of the type given in (1). The prototype is shown in Figure 3.

This Section is organized in two subsections, in the first one a general description of the laboratory prototype is given while the real-time obtained results are presented later.

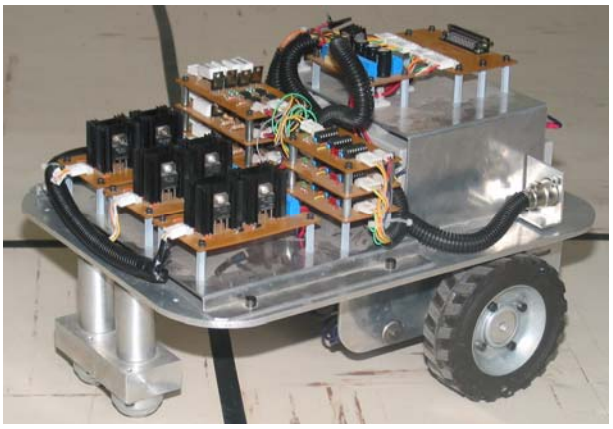

Fig. 3. Laboratory prototype

5.1 Prototype description

The experimental validation of the proposed control scheme has been carried out using a laboratory prototype of the type (1). The robot's wheels have a radius of $r = 6.5\,\text{cm}$ and are mounted on an axle of length $2l = 28.8\,\text{cm}$ between wheels. Two passive omnidirectional wheels are placed on the front part of the vehicle. The aluminium chassis measures $42 \times 32 \times 26\,\text{cm}$ (L/W/H) and supports two DC motors, reduction gears, power electronics, and a 12-V battery. Each motor has an incremental encoder counting $n_e = 1000\,\text{pulses/turn}$.

The prototype is controlled by a dSPACE Floating-Point Controller Board DS1102 that is based on the Texas

Instruments TMS320C31 DSP. This board is placed on a 1-GHz Pentium III PC, with control algorithms written in Matlab's SIMULINK. The dSPACE Control Desk software provides a GUI with real-time visualization. The Controller Board communicates through multi-wire cable with the electronics on the robot. The two wheels of the WMR are driven by PWM signals sent by the DS1102 Board and their encoders measure the angular displacements ϕ_r and ϕ_l on the motors for odometric computations.

The velocity control of the two motors is done by means of PID controllers implemented on the DS1102 Board. This controller features a Coulomb plus viscous friction compensation block. Filtering algorithms, potentiometer data adaptation and posture reconstruction from odometric data are implemented in the DS1102 Board. A general control scheme is shown in Figure 4.

The relationship between the longitudinal and angular velocity of the robot and the angular velocities of each wheel are given by,

$$\begin{bmatrix} \omega_r \\ \omega_l \end{bmatrix} = \begin{bmatrix} r/2 & r/2 \\ r/2l & -r/2l \end{bmatrix} \begin{bmatrix} u_1 \\ u_2 \end{bmatrix}$$

where ω_r and ω_l represent the angular velocity of right and left traction wheels.

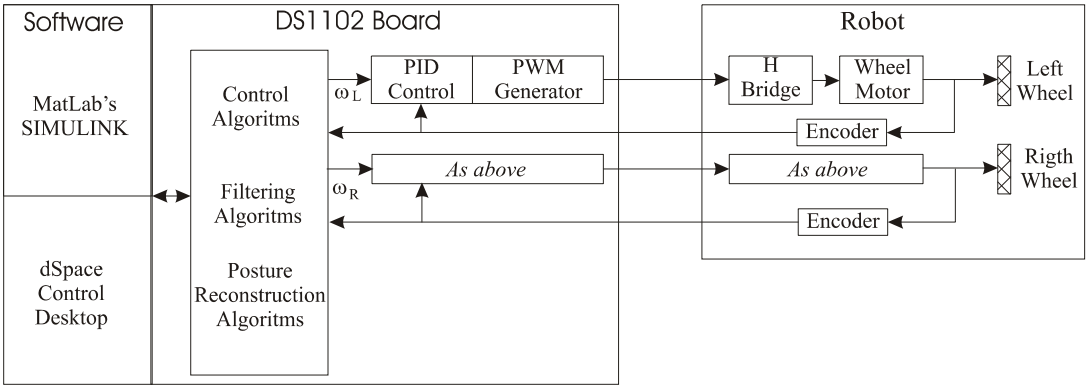

Fig. 4. General control scheme

5.2 Real-time experimental results

This Subsection is devoted to present the results obtained by the real-time implementation of the discrete-time control scheme (21) applied to the laboratory prototype described in the previous subsection. The experiments were carried out by considering the following coefficients for $\bar{v}$ and $\tilde{v}$ given in equations (14) and (19): $m_0 = \tilde{m}_0 = 0.0893$, $\bar{m}_1 = \tilde{m}_1 = 1.082$, $\bar{m}_2 = \tilde{m}_2 = 1.99$, $\bar{k}_0 = \tilde{k}_0 = 0.989$, $\bar{k}_1 = 1.989$.

In all the experiments it was considered a sampling period $T = 0.5s$; the commutation threshold given in equation (21) was taken as $\varepsilon = 0.05$ and the initial values for the state errors $e_1 = x_1 - x_{1d}$, $e_2 = x_2 - x_{2d}$, $e_3 = \theta_0 - \theta_{0d}$ were set to zero.

The prescribed trajectory is composed by two straight lines and a circumference arc (see Figure 5). This trajectory contains singular points for which the control law $\bar{w}$ is not well defined, allowing to evaluate the performance of the control scheme (21) by commutations between $\bar{w}$ and $\tilde{w}$. The mobile robot completes the desired trajectory in seventy seconds, the first twenty through the horizontal line, the next thirty through the circumference arc and the last twenty through the vertical line. It is assumed that for each segment of the trajectory the starting and ending points have velocity equal to zero.

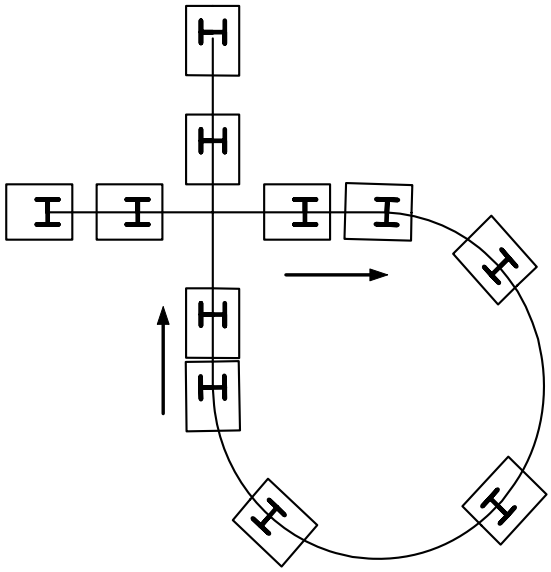

Fig. 5. Mobile robot following a prescribed trajectory

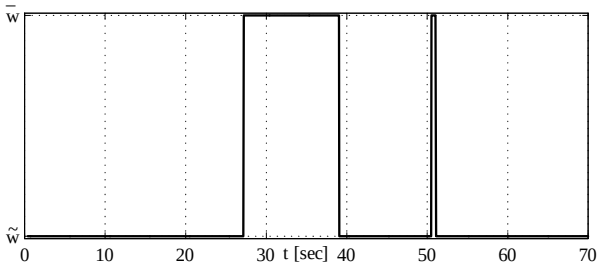

Fig. 6. Commutation between controls

The position on the workspace of the mobile robot at different sampling instants (each 7s) is shown in Figure 5. The initial position of the robot at the beginning of the desired trajectory is accordingly with the considered initial errors.

The commutation between the feedback laws $\bar{w}$ and $\tilde{w}$ is shown in Figure 6 where the alternation of the two control laws during the experiment is presented.

The evolution of the input signals w_1 and w_2 is shown in Figure 7 where it is possible to see that the commutation between the feedback laws $\bar{w}$ and $\tilde{w}$ does not influence the control signals w_1 and w_2. Some peaks can be observed at the points of the trajectory where the straight lines and the circumference arc are joined. These peaks are produced by the coulomb friction of the motors because the robot velocity is zero at these points.

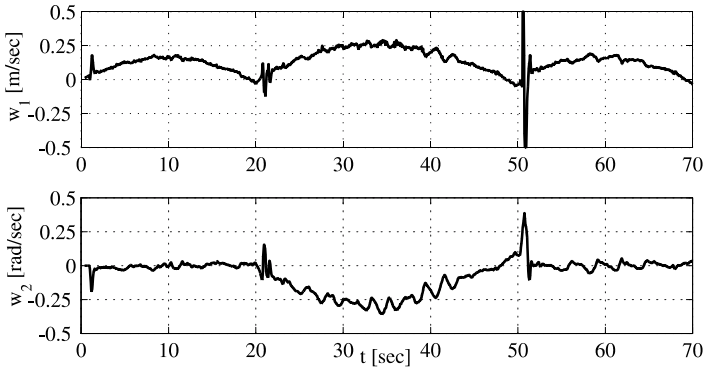

Fig. 7. Evolution of input signals w_1 and w_2

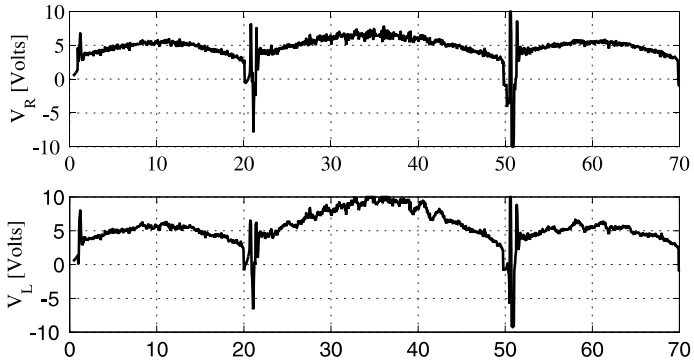

Fig. 8. Voltage applied to the right (V_R) and (V_L)

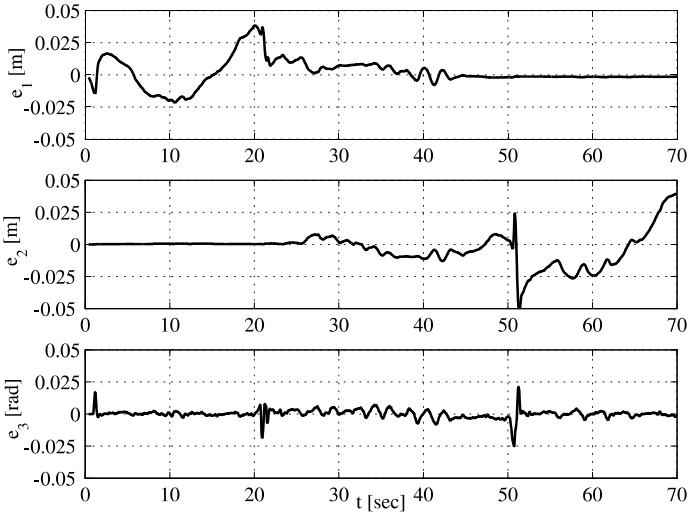

Fig. 9. Evolution of the state errors e_1, e_2, e_3

The voltage applied to each motor of the wheels is shown in Figure 8. Some peaks can be observed at the same times that the ones on the controllers (see Figure 7) as expected. These voltage signals are provided by the PID blocks that control the velocity of the wheel motors.

The evolution of the trajectory errors $e_1 = x_1 - x_{1d}$, $e_2 = x_2 - x_{2d}$, $e_3 = \theta_0 - \theta_{0d}$ is shown in Figure 9. The trajectory errors e_1 and e_2 have three different behaviors corresponding to each part of the trajectory. The state error e_3 (corresponding to the output error $\varepsilon_2 = \tilde{\varepsilon}_2$) is around zero as expected with small peaks at the trajectory joints.

6 Conclusions

The discrete-time model of a two-wheel differentially driven mobile robot is obtained by direct integration of its continuous-time model producing an exact discrete-time representation. This discrete-time model is used to design a control scheme that solves the path tracking problem. The output function commonly used to obtain a full linearizing control law for the same type of robot in continuous-time can not be longer applied for the discrete-time system. A new output function is proposed to obtain a full linearizing discrete-time controller. This new discrete-time controller has a singular manifold that does not allow to solve the path tracking problem for any desired trajectory. In order to obtain a globally defined control scheme, an alternative linearizing control law is designed with a different singular manifold. The second control law is enabled when the states are in a neighborhood of the singular manifold of the first one. The proposed commutation scheme that solves the path tracking problem is based on the commutation of these two discrete-time control laws. The performance of the proposed control strategy is evaluated by means of real time experiments carried out over a low cost laboratory prototype. The obtained results show good performance of the proposed control strategy and that the commutation between the considered feedbacks does not affect the evolution of the signals. The proposed control scheme guarantees that all internal signals remain bounded as is proved in this work.

Acknowledgement

First author work was partially supported by CONACyT-México, Under Grant 61713.

References

1. **Aranda-Bricaire E., Kotta U. and Moog C. H.** "Linearization of discrete-time systems", *SIAM Journal on Control and Optimization*, 34(6):1999–2023, 1996.
2. **Aranda-Bricaire E., Salgado-Jiménez T. and Velasco-Villa M.** "Control no lineal discontinuo de un robot móvil", *Computación y Sistemas*, Special Number:42–49, 2002.
3. **Campion G., Bastin G. and D'Andréa-Novel B.** "Structural properties and clasification of kinematics and dynamics models of wheeled mobile robots", *IEEE Transactions on Robotics and Automation*, 12(1):47–61, 1996.
4. **Canudas C., Siciliano B., Bastin G., Brogliato B., Campion G., D'Andrea-Novel B., De Luca A., Khalil W., Lozano R., Ortega R., Samson C. and Tomei P.** *Theory of Robot Control*. Springer-Verlag, London, 1996.
5. **Corradini M. L., Leo T. and Orlando G.** "Robust stabilization of a mobile robot violating the nonholonomic contraint via quasi-sliding modes", *Proccedings of the American Control Conference*, 3935–3939, USA, June 1999.
6. **Corradini M. L., Leo T. and Orlando G.** "Experimental testing of a discrete-time sliding mode controller for trajectory tracking of a wheeled mobile robot in the presence of skidding effects", *Journal of Robotics Systems*, 19(4):177–188, 2002.
7. **D'Andrea-Novel B., Bastin G. and Campion G.** "Dynamic feedback linearization of nonholonomic wheeled mobile robots", *Proceedings of the IEEE International Conference on Robotic and Automation*, 2527–2532, Nice, France, 1992.

8. **Isidori A.** *Nonlinear Control Systems*, Springer-Verlag, New York, 1995.
9. **Kotta U.** *Inversion Method in the Discrete-Time Nonlinear Control Systems*, Springer-Verlag, London, 1995.
10. **Nijmeijer H. and Van der Schaft A.** *Nonlinear Dynamical Control Systems*, Springer-Verlag, New York, 1990.
11. **Oelen W., Berghuis H., Nijmeijer H. and Canudas C.** "Hybrid stabilization control of a real mobile robot", *IEEE Robotics and Automation Magazine*, 2(2):16–23, 1995.
12. **Oriolo G., De Luca A. and Venditteli M.** "WMR control via dynamic feedback linearization: Design, implementation, and experimental validation", *IEEE Transaction on Control Systems Technology*, 10(6):835–852, 2002.
13. **Orosco-Guerrero R., Aranda-Bricaire E. and Velasco-Villa M.** "Global path-tracking for a multi-steered general n-trailer". *Proceedings 15th IFAC World Congress*, Barcelona, Spain, 2002.
14. **Orosco-Guerrero R., Aranda-Bricaire E. and Velasco-Villa M.** "Modeling and dynamic feedback linearization of a multi-steered general n trailer system", *Proceedings 15th IFAC World Congress*, Barcelona, Spain, 2002.
15. **Wargui M., Tadjine M. and Rachid A.** "Stability of real time control of an autonomous mobile robot", *IEEE 5th. International Workshop on Robot and Human Communication*, 311–316, Tsukuba, Japan, November 1996.
16. **Wargui M., Tayebi A., Tadjine M. and Rachid A.** "On the stability of an autonomous mobile robot subject to network induced delay", *IEEE International Conference on Control Applications*, 28–30, Hartford, CT, October 1997.

Martín Velasco Villa *is a Professor at the Electrical Engineering Department of the Research and Advanced Studies Center of the National Polytechnic Institute (CINVESTAV-IPN). He obtained his M. Sc and Ph. D. Degrees at CINVESTAV-IPN, in 1989 and 1994 respectively. His main interests are focused on the analysis and control of time delay systems as well as mobile robotic systems.*

Eduardo Aranda Bricaire *was born in Mexico City. He received the M. Sc. degree from the Research and Advanced Studies Center of the National Polytechnic Institute (CINVESTAV-IPN), Mexico, in 1991, and the Ph. D. degree form Ecole Centrale de Nantes and the University of Nantes, France, in 1994. Since then he has been with the Electrical Engineering Department at CINVESTAV-IPN and was appointed Full Professor in 1997. He has held visiting positions at Queen's University, Kingston, Canada, the Institute of Information Theory and Automation of the Academy of Sciences of the Czech Republic, the Institute of Research on Communications and Cybernetics of Nantes, France, and the Mexican Institute of Petroleum. He is a Regular Member of the Mexican Academy of Sciences. Dr. Aranda-Bricaire served as President of the Mexican Association of Automatic Control (the corresponding IFAC*

NMO) during the term 2006-2007. His research interests include the analysis and control of nonlinear systems and mobile robotics.

Rodolfo Orosco Guerrero *is a full professor and researcher of the Instituto Tecnológico de Celaya assigned to the Electronics Department since 1992. He got his PhD from the Electrical Engineering Department at CINVESTAV-IPN, Mexico. Currently he is with the Master Degree Program teaching several courses in the area of digital control, Industrial automation and analog electronics. His current research works are oriented to navigation of wheeled mobile robots and digital controls of power electronics circuitry. He belongs to the "quality of energy" research area.*